Study of SOD Mimic and Nucleic Acid Interaction Activity Exerted by Enrofloxacin-Based Copper(II) Complexes

by **Mohan N. Patel***, **Bhupesh S. Bhatt**, and **Promise A. Dosi**

Department of Chemistry, Sardar Patel University, Vallabh Vidyanagar–388120, Gujarat, India (phone: (+912692)226856*218; e-mail: jeenen@gmail.com)

Five new copper(II) complexes of type [Cu(erx)(**L**)Cl] (erx, enrofloxacin; thiophene-2-carbaldehyde (**L**^{1}); pyridine-2-carbaldehyde (**L**^{2}); 2,2′-dipyridylamine (**L**^{3}); 4,5-diazafluoren-9-one (**L**^{4}); bis(3,5-dimethyl-1-pyrazolyl)methane (**L**^{5})) have been synthesized and characterized by elemental analysis, reflectance, IR, and FAB-MS. Complexes have been investigated for their interaction with calf thymus (CT) DNA utilizing the absorption-titration method, viscometric and DNA thermal denaturation studies. The cleavage reaction on pUC19 DNA has been monitored by agarose gel electrophoresis. The results indicated that the Cu^{II} complexes can more effectively promote the cleavage of plasmid DNA at physiological pH and superoxide dismutase. The (SOD) activity of the complexes has been evaluated by the nitroblue tetrazolium assay, and the complexes catalyzed the dismutation of superoxide at pH 7.8 with IC_{50} values of 0.35–1.25 μM. The complexes have also been screened for their antibacterial activity against five pathogenic bacteria.

Introduction. – The study of DNA–metal interactions constitutes a growing research area. In addition to their potential use as therapeutic agents, they are being considered as tools for biochemistry and molecular biology [1]. DNA plays an important role in the life process, because it bears genetic information and instructs the biological synthesis of proteins and enzymes through the replication and transcription of genetic information in living cells. DNA is a particularly good target for metal complexes, as it offers a wide variety of potential metal-binding sites [2–5]. Such sites include the electron-rich DNA bases or phosphate groups that are available for direct covalent coordination to the metal center. There are noncovalent binding modes as well, such as H-bonding and electrostatic binding to grooved regions of the DNA and intercalation of planar aromatic ligands into the stacked base pairs.

Copper is found in a variety of enzymes, including the Cu-centers of cytochrome-c oxidase and the enzyme superoxide dismutase (SOD; containing Cu and Zn), and is the central metal in the oxygen-carrying pigment hemocyanin. In addition to its enzymatic roles, Cu is used for biological electron transport. Copper-superoxide dismutase (Cu-SOD) is believed to protect the cell against oxidative damage and inflammation due to toxic oxygen intermediates by the catalytic dismutation of superoxide radicals to O_2 molecules and H_2O_2 [6].

Fluoroquinolone antibacterial agents represent a fast-growing group of antibiotics; various derivatives were synthesized and tested for their antimicrobial activities. The new generations of fluoroquinolones achieved significant improvement in potency, spectrum, and physicochemical properties [7]. 'Quinolones' is a term commonly used

for the quinolonecarboxylic acids or 4-quinolones, a group of synthetic antibacterial agents containing a 1,4-dihydro-4-oxoquinoline skeleton [8–10]. Quinolones are extremely useful for the treatment of diverse infections [11–13]. The activity of quinolones as antibacterial drugs is due to the effective inhibition of DNA replication. The proposed mechanism of the interaction between quinolone and metal ions was chelation between the metal, and the 4-oxo and adjacent COOH groups [14]. Enrofloxacin is a typical second-generation quinolone antimicrobial drug with a broad spectrum of activity against a wide range of *Gram*-negative and *Gram*-positive bacteria, including those resistant to β-lactam antibiotics and sulfonamides [15][16]. It is also used for the treatment of urinary-tract infections, pyelonephritis, sexually transmitted diseases, prostatitis, skin and tissue infections, and urethral and cervical gonococcal infections [17–19]. Due to such biological activities of enrofloxacin and extensive bioavailability of Cu^{II}, we have synthesized five mononuclear Cu^{II} complexes with enrofloxacin and different heterocyclic units expecting that coordination could enhance the biological activity of enrofloxacin by increasing lipophilicity of the drug.

This article mainly focuses on exploring the trend in DNA-binding affinities of complexes and the important differences in some related properties. Understanding the features that contribute to recognition of DNA by small ligands or metal complexes is crucial for the development of drugs targeted at DNA.

Results and Discussion. – *Characterization of Complexes.* All the complexes were characterized using elemental analysis, conductance, magnetic measurements, reflectance, and IR and FAB-MS. The elemental analysis is in accordance with the proposed 1:1:1 metal/erx/**L**^{n} ratio. The molar-conductance values were determined as described by *Kulkarni et al.* using DMF as solvent [20]. The conductance values were too low to account for presence of any hydrolyzable chloride ions in complexes, indicating the nonelectrolytic nature of the complexes.

The diffuse reflectance spectra of Cu^{II}–enrofloxacin complexes consist of one asymmetric broad band center around 15,000 cm^{-1} for all the compounds, characteristic of distorted square-pyramidal geometry [21].

The observed magnetic moments of Cu^{II} complexes are given in *Table 1*. The best compilation of the results on the magnetic behavior of Cu compounds was provided by *Figgis, Nyholm*, and co-workers [22]. At room temperature, the magnetic moments of the complexes lie in the range of 1.81–1.90 B.M., which is higher than the spin-only value of 1.73 B.M.

A comparison of the IR spectra of the complexes with those of the free ligands revealed interesting features related to the metal–ligand interactions. In the IR spectrum of enrofloxacin, the valence vibration of the carboxylic stretch ν(C=O) was found at 1733 cm^{-1} and the pyridone stretch ν(C=O) at 1622 cm^{-1}. The characterization of quinolone metal complexes could be achieved by studying the most typical vibrations that are characteristic of the coordination type of quinolones. In *Table 2*, the characteristic absorptions in the IR spectra of the complexes are collected. In the IR spectra of the complexes **1**–**5**, the absorption at ν(C=O) is replaced by two very strong characteristic bands in the range of 1559–1578 and 1348–1374 cm^{-1} assigned to asymmetric ($\nu(COO)_{as}$) and symmetric ($\nu(COO)_s$) vibrations. The difference $\Delta = \nu(COO)_{as} - \nu(COO)_s$ is a useful characteristic for determining the coordination mode

Table 1. *Experimental and Physical Parameters of the Complexes*

Empirical formula	Formula weight [g/mol]	Elemental analysis [%] found (calc.)				M.p. [°]	Yield [%]	μ_{eff} [B.M.]	Λ_m [Ohm^{-1} cm^2 mol^{-1}]
		C	H	N	M				
$C_{24}H_{25}ClCuFN_3O_4S$	569.54	50.54 (50.61)	3.42 (3.39)	7.45 (7.38)	11.12 (11.16)	220	69.3	1.81	22.1
$C_{25}H_{26}ClCuFN_4O_4$	564.50	53.13 (53.19)	4.60 (4.64)	9.88 (9.93)	11.31 (11.26)	219	67.9	1.88	21.9
$C_{29}H_{30}ClCuFN_6O_3$	628.58	55.46 (55.41)	4.73 (4.81)	13.44 (13.37)	10.06 (10.11)	221	65.4	1.85	22.2
$C_{30}H_{27}ClCuFN_5O_4$	639.56	56.30 (56.34)	4.21 (4.26)	10.90 (10.95)	9.90 (9.94)	243	67.4	1.83	22.6
$C_{32}H_{39}ClCuFN_5O_3$	659.68	58.22 (58.26)	5.87 (5.96)	10.56 (10.62)	9.56 (9.63)	235	65.2	1.90	20.9

Table 2. *IR-Spectral Data of Complexes and Enrofloxacin*

Compounds	ν(C=O) [cm^{-1}] of pyridone	$\nu(COO)_{asy}$ [cm^{-1}]	$\nu(COO)_{sym}$ [cm^{-1}]	$\Delta\nu$ [cm^{-1}]	ν(M–N) [cm^{-1}]	ν(M–O) [cm^{-1}]
Enrofloxacin	1733	1622	1340	284	–	–
Complex **1**	1621	1561	1359	202	532	507
Complex **2**	1619	1578	1374	204	535	506
Complex **3**	1618	1569	1371	198	538	510
Complex **4**	1621	1569	1355	214	545	511
Complex **5**	1617	1559	1348	211	541	513

of the ligands. The Δ values fall in the range of 202–214 cm^{-1} indicating a monodentate coordination mode of the carboxylato group [23–27]. The pyridone stretch, ν(C=O), is slightly shifted from 1617 to 1621 cm^{-1} upon bonding. The overall changes of the IR spectra indicate that enrofloxacin is coordinated to the metal *via* the pyridone and one carboxylate O-atoms.

All the synthesized complexes show the molecular-ion peaks associated with different number of H-atoms. *Fig. 1* represents the FAB-MS of [Cu(erx)(L^1)Cl] (**1**), obtained using 3-nitro-benzyl alcohol as matrix. Peaks at *m*/*z* 136, 137, 154, 289, and 307 are due to the matrix. *Doublets* appeared at 568, 570; 456, 458; and 209, 211 for the fragments with a single Cl-atom, respectively. Loss of the Cl-atom gave a fragment-ion peak at *m*/*z* 533, which also confirms that the Cl-atom was attached to metal ion with covalent bond. Several other peaks for fragments with *m*/*z* 421, 359, 174, and 112 were also detected. Similar patterns were also observed for the other synthesized complexes.

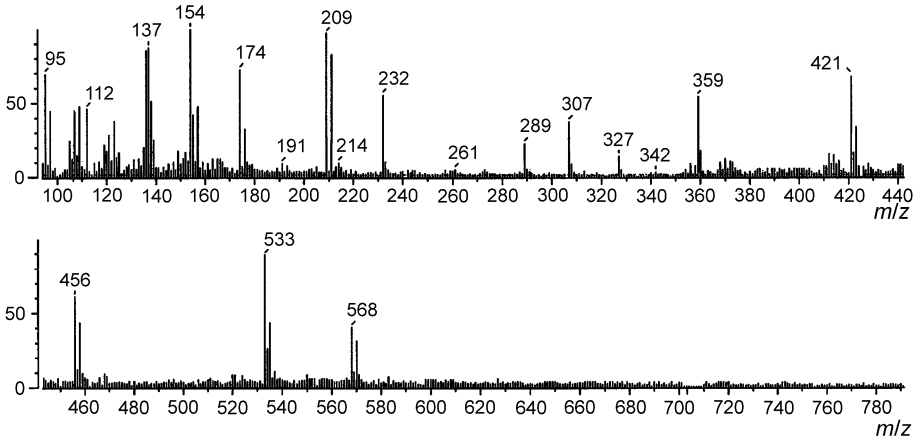

Fig. 1. *FAB Mass spectrum of [Cu(erx)(***L^1***)Cl]* (**1**) *obtained using* 3*-nitrobenzyl alcohol*

Antibacterial Activity. The efficiency of the ligands and the complexes have been tested against three *Gram*-negative (*Escherichia coli*, *Serratia marcescens*, and *Pseudomonas aeruginosa*) and two *Gram*-positive (*Staphylococcus aureus* and *Bacillus subtilis*) microorganisms. The results of the minimum inhibitory concentration (*MIC*)

Table 3. MIC *Data of the Compounds* [μM]

Compounds	*S. aureus*	*B. subtilis*	*S. marcescens*	*P. aeruginosa*	*E. coli*
$CuCl_2 \cdot 2\ H_2O$	2698.00	2815.00	2756.00	2404.00	3402.00
Enrofloxacin	1.9	3.9	1.7	1.4	1.4
Complex **1**	1.0	2.1	1.3	1.4	0.7
Complex **2**	0.7	1.2	0.7	1.2	0.3
Complex **3**	0.5	1.5	0.9	1.2	0.5
Complex **4**	1.2	1.7	0.8	0.9	0.8
Complex **5**	0.9	1.9	0.7	1.1	0.7

expressed in μM are presented in *Table 3*. All compounds exhibited good activities against all microorganisms compared to reference drugs. The complexes showed better antimicrobial activities than the corresponding free ligands and enrofloxacin. The higher antimicrobial activities can be mainly attributed to the presence of the quinolone chelated with the complexes. Comparing the results with those of the previously reported Cu^{II} complexes of pefloxacin and sparfloxacin with similar ligands L^1, L^2, and L^3 [26], we can state that replacement of pefloxacin and sparfloxacin with enrofloxacin enhances antibacterial activities of all compounds except for $[Cu(PFL)(A^2)Cl] \cdot 5\ H_2O$ against *P. aeruginosa* and *E. coli*.

Chelation reduces the polarity [28][29] of the metal ion mainly because of the partial sharing of its positive charge with the donor groups and possibly the π- electron delocalization within the whole chelate ring system thus formed during coordination. This process of chelation increases the lipophilic nature of the central metal atom, which in turn favors its permeation through the lipoid layer of the membrane, increasing the hydrophobic character and liposolubility of the molecule in crossing cell membrane of the microorganism, and hence enhances the biological utilization ratio and activity of the tested drugs/compounds.

In addition, our study regarding bactericidal activity in terms of colony-forming units (CFU)/ml of the metal complexes against same microorganisms revealed decrease in number of colonies with increasing concentration of compounds. The results are shown in *Fig. 2* for all the complexes against *S. aureus*. The number of colonies counted in this technique was 30–250 CFU/ml.

DNA-Binding Properties. Electronic absorption spectroscopy is employed to determine the binding characteristics of metal complex with DNA. *Fig. 3* shows the absorption spectra of complex **1** in the presence of increasing amounts of calf thymus (CT) DNA. Absorption titration experiments of Cu^{II} complexes in buffer were performed using a fixed copper concentration to which increments of the DNA stock solution were added. The binding of Cu^{II} complexes to duplex DNA led to decrease in the absorption intensities with a small amount of red shifts in the UV/VIS absorption spectra. In the UV region, the intense absorption bands observed in the Cu^{II} complexes are attributed to the intraligand $\pi-\pi^*$ transition of the coordinated groups. Addition of increasing amounts of CT-DNA resulted in hypochromism and bathochromic shift in the UV spectra of all complexes due to intercalative mode involving a strong stacking interaction between an aromatic chromophore and the nucleobases of DNA base stack [30].

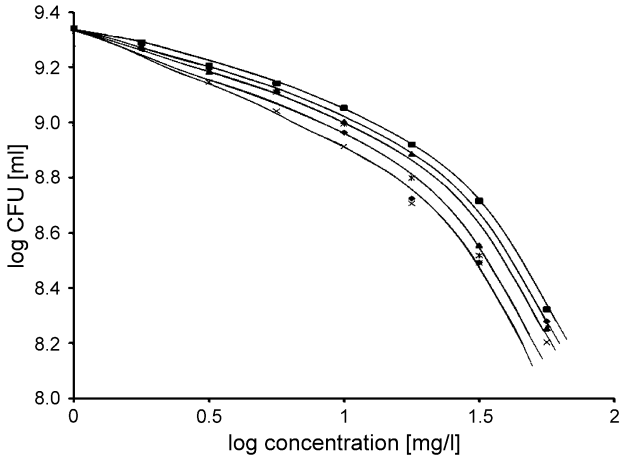

Fig. 2. *Relationship between concentration and bactericidal activity of all complexes against* S. aureus (CFU, colony-forming unit)

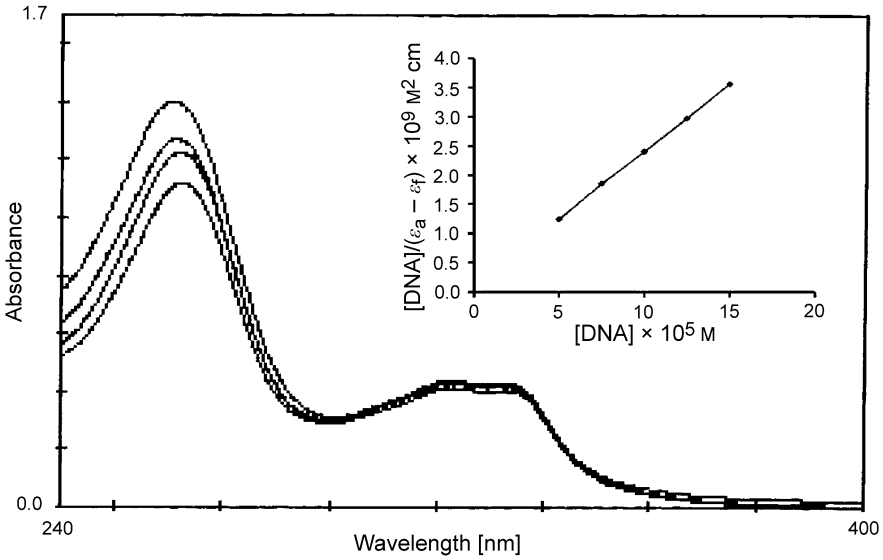

Fig. 3. *Electronic absorption titration curve of [Cu(erx)(*$\mathbf{L}^1$*)Cl] in absence and in presence of increasing amount of CT-DNA in 5 mM* Tris·*HCl buffer* (pH 7.2). [Complex] = 15 μM, [DNA] = 50–150 μM with an incubation period of 30 min. at 27°. *Inset:* Plot of $[DNA]/(\varepsilon_a - \varepsilon_f)$ *vs.* [DNA].

The binding constants (K_b) of complexes are calculated in the range of 1.17×10^4–2.96×10^4 M^{-1} (*Table 4*). The K_b values of metal complexes were greater than those previously reported for Cu^{II} complexes of pefloxacin and sparfloxacin except for $[Cu(PFL)(A^3)Cl] \cdot 5\,H_2O$ [26]. Comparing the intrinsic binding constant of complexes

with that of the DNA-intercalative $[Ru(bpy)_2ppd]^{+2}$ (1.18×10^4 M^{-1}) complex [31], we can deduce that all of the complexes bind moderately to DNA by intercalation. The K_b values of complexes **1**–**5** are greater than those of Cr^{III} and Cr^{IV} complexes reported by *Guo et al.* [32], comparable to those of Fe^{III} and Co^{II} complexes reported by *Psomas* [33], and Zn^{II} complexes reported by *Kessissoglou* and co-workers [34] while lower than those of Zn^{II} complexes reported by *Kessissoglou* and co-workers [35]. The spectral characteristics obviously indicate that the metal complexes interact with DNA most likely through intercalation mode.

Table 4. *Binding Constants, and* IC_{50} *and* LC_{50} *Values of* Cu^{II} *Complexes*

Complexes	K_b [M^{-1}]	IC_{50} [μM]	LC_{50} [μM]
[Cu(erx)(**L**^{1})Cl] (**1**)	1.94×10^4	0.50	21.06
[Cu(erx)(**L**^{2})Cl] (**2**)	2.96×10^4	0.35	21.70
[Cu(erx)(**L**^{3})Cl] (**3**)	1.52×10^4	1.00	14.51
[Cu(erx)(**L**^{4})Cl] (**4**)	1.17×10^4	1.25	12.71
[Cu(erx)(**L**^{5})Cl] (**5**)	1.68×10^4	0.75	9.56

To further clarify the nature of the interactions between the complexes and DNA, viscosity measurements were carried out. Optical and photophysical probes provide necessary, but not sufficient evidence to support the model of binding of the Cu^{II} complexes with DNA. Hydrodynamic measurements that are sensitive to length change (*i.e.*, viscosity) are regarded as the least ambiguous and the most critical tests of a binding model in solution in the absence of crystallographic structural data [36][37]. Intercalation is expected to lengthen the DNA helix, as the base pairs are pushed apart to accommodate the bound ligand, leading to an increase in the DNA viscosity. In contrast, a partial, non-classical intercalation of the ligand could bend (or kink) the DNA helix, reduce its effective length and, concomitantly, its viscosity. The effects of complexes, together with enrofloxacin and ethidium bromide (EB), on the viscosity of rod-like DNA are shown in *Fig. 4*. The well-known DNA intercalator EB increases the viscosity of DNA with increments of the concentration. Upon increasing the amount of complexes, the relative viscosity of DNA increased steadily, but less than with EB. The increase of the relative viscosity, expected to correlate with the DNA-intercalating potential of a compound, follows the order EB $>$ **2** $>$ **1** $>$ **5** $>$ **3** $>$ **4** $>$ enrofloxacin. The results are consistent with previously reported metal complexes of type [Cu(PFL/SPFL)(A^n)Cl]·5 H_2O [26]. These results suggest that all the title complexes intercalate between the base pairs of DNA, with the difference in binding strength probably being caused by the different substituent on ancillary ligands.

The thermal behavior of DNA in the presence of complexes can provide insight into their conformational changes when the temperature is raised, and offer information about the interaction strength of the complexes with DNA. It is well-known that, when the temperature of the solution is increased, the double-stranded DNA gradually dissociates to single strands, generating a hyperchromic effect in the absorption spectra of the DNA bases (λ_{max} 260 nm). To identify this transition process, the melting temperature, T_m, which is defined as the temperature where half of the total base pairs are unbonded, is usually determined. According to the literature [38][39], the

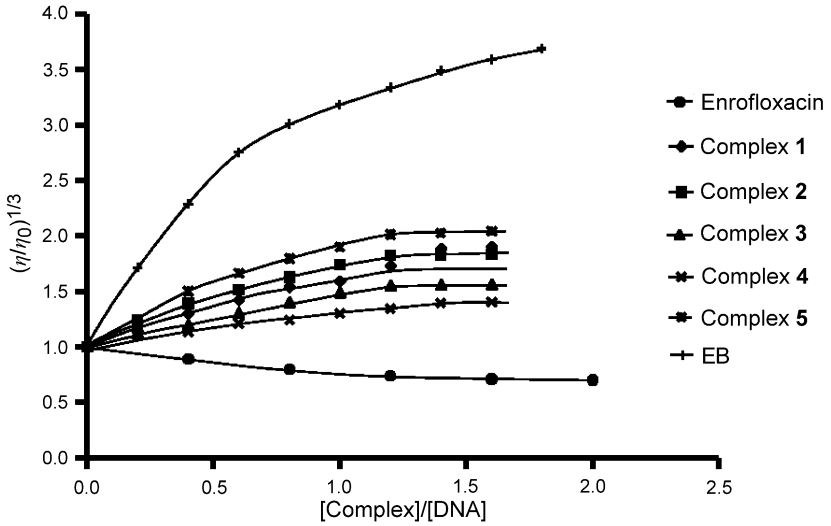

Fig. 4. *Relative viscosity of DNA under the influence of increasing amounts of complexes at 27±0.1° in 5 mM* Tris·*HCl buffer* (pH 7.2) *as a medium*

intercalation of metallo-intercalators generally results in a considerable increase of T_m. The melting curves of CT-DNA in the absence and presence of the complexes are presented in *Fig. 5*. Here, the thermal denaturation experiment carried out for DNA in the absence of the Cu^{II} complexes revealed a T_m value of 74.2° under our experimental conditions. On addition of complexes **1**–**5**, T_m of DNA increased to 79.2, 79.5, 78.4, 78.1, and 78.9°, respectively, at a concentration ratio [DNA]/[Cu] of 5:1. The large increase, *i.e.* 3.9–5.3, in T_m values is comparable to that observed for classical intercalators.

DNA-Cleavage Study. There has been considerable interest in nucleolytic cleavage reactions that are activated by complexes [40–42]. The ability of the all metal complexes to cleave DNA has been investigated by gel electrophoresis using pUC19 DNA. The cleavage of plasmid pUC19 DNA was monitored by gel electrophoresis to investigate the ability of the present Cu^{II} complexes to serve as metallonucleases (*Fig. 6*). The naturally occurring supercoiled form (Form I), when nicked, gives rise to an open circular relaxed form (Form II) and further cleaves to a linear form (Form III). When subjected to gel electrophoresis, Form I shows the fastest migration compared to Forms II and III. Form II migrates very slowly prior to its relaxed structure, whereas Form III migrates somewhere between the positions of Form I and II [43]. The quantitative study of DNA cleavage in different forms is compiled in *Table 5*.

Superoxide Dismutase (*SOD*). The mixed-ligand Cu^{II} complexes were synthesized as a model for the active site of Cu-SOD. The SOD-like activities of the complexes were investigated by nitroblue tetrazolium (NBT) assay and catalytic activities toward the dismutation of superoxide anion were measured. The complexes provide a stable environment similar to that in the active site in the native enzyme, ensuring the stable

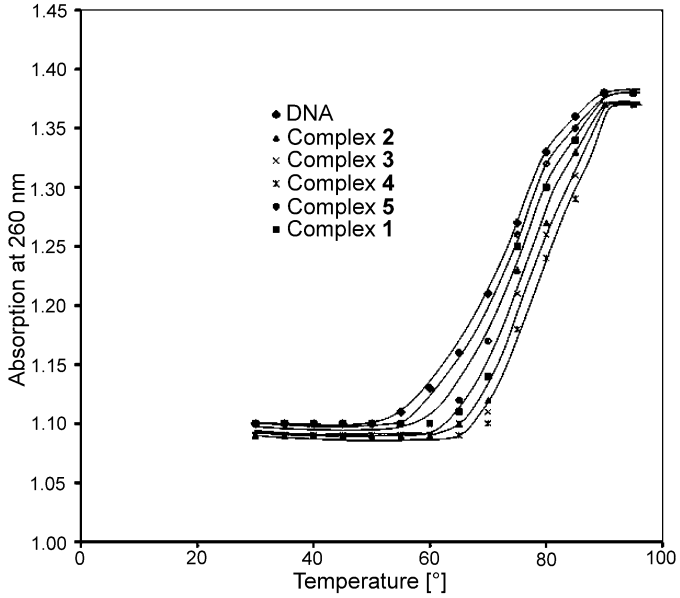

Fig. 5. *Melting curves of CT-DNA in the absence and presence of complexes* **1**–**5**

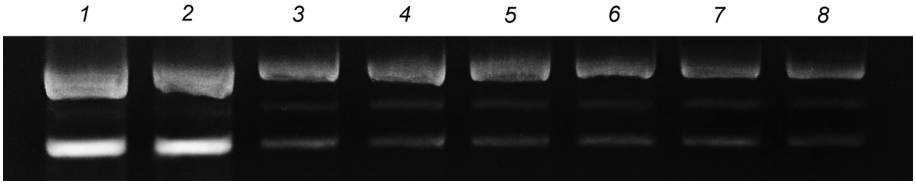

Fig. 6. *Interaction of pUC19 DNA* (300 μg/ml) *with a series of* Cu^{II} *complexes* (200 μM). *Lane 1*, DNA control; *Lane 2*, $CuCl_2 \cdot 2\,H_2O$; *Lane 3*, enrofloxacin; *Lane 4*, [Cu(erx)(**L**^{1})Cl]; *Lane 5*, [Cu(erx)(**L**^{2})Cl]; *Lane 6*, [Cu(**L**^{3})(erx)Cl]; *Lane 7*, [Cu(erx)(**L**^{4})Cl]; *Lane 8*, [Cu(erx)(**L**^{5})Cl].

Table 5. *Gel-Electrophoresis Data*

Compounds	% SC	% OC	% L
DNA control	77	23	–
DNA + Metal salt	75	25	–
DNA + Enrofloxacin	45	34	11
DNA + **1**	29	43	28
DNA + **2**	28	48	24
DNA + **3**	30	49	21
DNA + **4**	26	48	26
DNA + **5**	27	49	25

existence of the complex at the investigated pH value in aqueous solution. In this work, the SOD-like activities were measured at pH 7.8. The percentage inhibition of formazan formation at various concentrations of complexes as a function of time was

determined by measuring the absorbances at 560 nm and plotted to give a straight line (*Fig. 7*); with increase in concentration of tested complexes, a decrease in slope [*m*] was observed. The relationship between the inhibition [%] and initial concentration of the complex is depicted in *Fig. 8*.

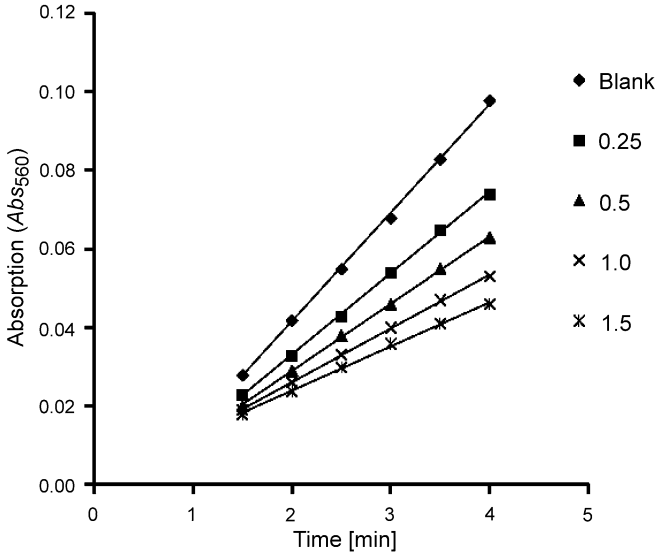

Fig. 7. *Absorbance values* (Abs_{560}) *vs. time* (*t*) *at different concentrations* [μM] *of complex* **1**

Compounds exhibited SOD-like activities at biological pH with the IC_{50} values in the range 0.35 to 1.25 μM. The superoxide scavenging data (*Table 4*) suggest that the complexes **1**–**5** have higher activity than those of the reported complexes of type [Cu(sftz)$(py)_3$Cl] [44]. The chromophore concentration required to yield 50% inhibition of the reduction of NBT (IC_{50}) was determined as described in [45]. Complexes **1**, **2**, and **5** have better radical scavenging activities than previously reported metal complexes of pefloxacin and sparfloxacin [26]. The result is reasonable, because the complexes **1**, **2**, and **5** are square planar with vacant coordination site, and the Cu-center is accessible to $O_2^{-}\cdot$.

Cytotoxocity. Brine shrimp lethality bioassay is a recent development in the assay procedure of bioactive compound, which indicates cytotoxicity as well as a wide range of pharmacological activities (such as anticancer, antiviral, insecticidal, pesticidal, AIDS, *etc.*) [46][47]. All the synthesized compounds were screened for their cytotoxicity (brine shrimp bioassay) according to the protocol of *Meyer et al.* [46]. From the data presented in *Table 4*, it is evident that compounds **4** and **5** displayed most potent cytotoxic activities against *Artemia* cysts, while the others were almost moderately active.

Conclusions. – The molecular-ion peaks in FAB-mass spectra for metal complexes account for attachment of neutral heterocyclic ligand, mono-anionic enrofloxacin, and

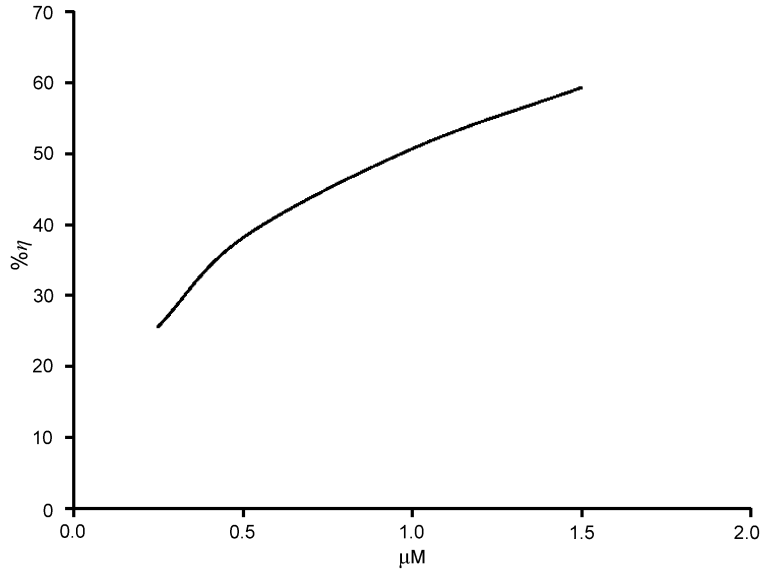

Fig. 8. *Percentage of inhibition of NBT* (nitroblue tetrazolium) *reduction* vs. *concentration of complex* **1**

Cl-atom in 1:1:1 ratio. IR-Spectral data suggest that monoanionic enrofloxacin is coordinated to the metal *via* the pyridone and one carboxylate O-atoms. Furthermore, conductance indicate the absence of any hydrolyzable Cl^- ion and also nonelectrolytic nature of metal complexes. The square pyramidal geometry suggested by reflectance spectra can only be possible if Cl^- ion is attached *via* covalent bond to the Cu^{II} in the metal complex making it neutral. The DNA-binding experiments suggest classical intercalation modes of binding. Nucleolytic experiments show sufficient interaction of metal complexes with DNA and hence support the DNA-binding data. The brine shrimp lethality assay shows the potent cytotoxic nature of the compounds. The SOD-like activity indicates the ability of metal complexes to scavenge free radical anions at their vacant coordination site. The SOD-mimic ability of title metal complexes is even higher than some known systems.

Experimental Part

General. All the chemicals and solvents were reagent-grade and used as purchased. Enrofloxacin hydrochloride was purchased from *Bayer AG* (D-Wuppertal). $CuCl_2 \cdot 2\,H_2O$, thiophene-2-carbaldehyde (**L**^{1}), pyridine-2-carbaldehyde (**L**^{2}), 2,2′-dipyridylamine (**L**^{3}), and CT-DNA were purchased from *Sd fine chemicals*, India. Ethidium bromide (EB) and *Luria Broth* were purchased from *Himedia*, India. AcOH and ethylenediaminetetraacetic acid (EDTA) were purchased from *Sd fine chemicals*, India.

Metal contents of the complexes were analyzed gravimetrically and volumetrically [48], after decomposing the org. matter with acid mixture ($HClO_4$, H_2SO_4, and HNO_3). C, H, and N elemental analyses: *Perkin-Elmer 240* elemental analyzer. Magnetic moments were measured by *Gouy*'s method using mercury tetrathiocyanatocobaltate(II) as the calibrant ($\chi_g = 16.44 \times 10^{-6}$ cgs units at 20°), on *Citizen* Balance. The diamagnetic correction was made using *Pascal*'s constant. The molar-conductance measurements were carried out on *Equip-Tronics EQ-660A*, conductivity meter (India). IR Spectra: *FT-*

IR Shimadzu spectrophotometer with sample prepared as KBr pellets in the range 4000–400 cm^{-1}. Reflectance spectra: *LAMBDA 19 UV/VIS/NIR* spectrophotometer, *Perkin-Elmer* (USA). FAB-MS: *Jeol SX 120/Da-600* mass spectrometer/data system using Ar/Xe (6 kV, 10 mA) as the FAB gas; the accelerating voltage was 10 kV, and spectra were recorded at r.t.

Syntheses. The ligands 4,5-diazafluoren-9-one (=5*H*-cyclopenta[1,2-*b*:5,4-*b*′]dipyridin-5-one; **L⁴**) and bis(3,5-dimethyl-1-pyrazolyl)methane (=1,1′-methanediylbis(3,5-dimethyl-1*H*-pyrazole); **L⁵**) were synthesized according to literature methods [49][50].

The metal complex **1** was prepared by adding MeOH soln. of $CuCl_2 \cdot 2\,H_2O$ (0.170 g, 0.001 mol) to MeOH soln. of thiophene-2-carbaldehyde (**L¹**) (0.112 g, 0.001 mol), followed by MeOH soln. of enrofloxacin (0.374 g, 0.001 mol), while adjusting pH to 6.8. The resulting soln. was refluxed for 2 h on a H_2O bath, followed by concentrating it to half of its volume. A fine amorphous product of green color was obtained which was washed with Et_2O/hexane and dried in vacuum desiccators. The proposed reaction is shown in the *Scheme*, and physical parameter of all the complexes are collected in *Table 1*. Remaining complexes **2**–**5** were prepared by following the process described above.

Scheme. *Formation of Complex [Cu(erx)(**L¹**)Cl]* (**1**)

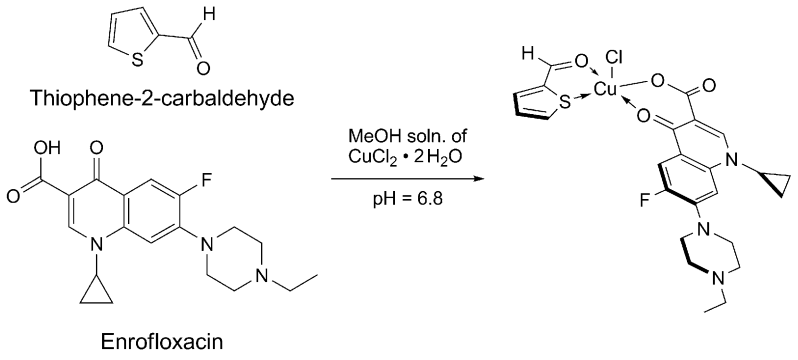

In vitro *Antibacterial Assay.* Antibacterial screening on different bacterial strains was performed by determining the minimum inhibitory concentration (*MIC*).The *MIC* value was defined as the lowest concentration of antimicrobial agent showing complete inhibition of growth. The *MIC* values of the reference drugs (ligands) were compared with those of the complexes. All cultures were incubated at 37°. Control tests with no active ingredients were also performed. The double dilution method was used for *MIC* determination.

The bactericidal activities of all compounds were also evaluated against the same bacterial culture. The inoculum was prepared by diluting a culture grown overnight in *Luria Broth* to obtain 10^6 viable bacteria/ml, confirmed in each experiment by colony counts. Bacteria were exposed to concentrations of 0.25–1.75 μg ml^{-1} of compounds. The final volume was 1 ml. Cultures were incubated at 37° for 2 h. The 100-μl bacterial cultures were taken and spread over previously prepared agar plates. These were incubated for 24 h at 37°, and the visual colonies were calculated in order to check biocidal activity of metal complexes, yielding 30–250 colonies.

DNA-Binding Experiments. Viscosity Measurements. Viscosity experiments were carried on an *Ubbelohde* viscometer, immersed in a thermostatic H_2O-bath maintained at a constant temp. of $27 \pm 0.1°$. DNA Samples of *ca.* 200 base pairs in average length were prepared by sonication in order to minimize complexities arising from DNA flexibility [51]. Data were presented as $(\eta/\eta_0)^{1/3}$ *vs.* binding ratio [52], where η is the viscosity of DNA in the presence of complex, and η_0 is the viscosity of DNA alone. Viscosity values were calculated from the observed flow time, t, of DNA-containing solns., t was corrected for that of buffer alone, t_0, $\eta = (t - t_0)$.

Absorption Titration. Solns. of DNA in the buffer gave a ratio at UV absorbances at 260 and 280 nm, A_{260}/A_{280}, of 1.9, indicating that the DNA was sufficiently free of protein. The concentration of DNA was

determined from the band intensity at 260 nm with a known extinction coefficient value ($\varepsilon_{260}=6600\,\text{M}^{-1}\,\text{cm}^{-1}$). Absorption titration measurements were carried out by varying the concentration of CT-DNA from 50 to 150 μM, while keeping the metal-complex concentration constant at 15 μM in the buffer soln. Samples were incubated at 37° for 24 h before recording each spectrum. The intrinsic binding constant (K_b) for the interaction of the complexes with CT-DNA was determined from a plot of [DNA]/($\varepsilon_a-\varepsilon_f$) *vs.* [DNA] using absorption spectral titration data and the following equation [53]:

$$\frac{[\text{DNA}]}{(\varepsilon_a-\varepsilon_f)}=\frac{[\text{DNA}]}{(\varepsilon_b-\varepsilon_f)}+\frac{1}{K_b(\varepsilon_b-\varepsilon_f)} \tag{1}$$

where [DNA] is the concentration of DNA, the apparent absorption coefficients ε_a, ε_f, and ε_b correspond to A_{obs}/[Cu], the extinction coefficient for the free Cu^{II} complex, and the extinction coefficient for the Cu^{II} complex in the fully bound form, resp. The K_b value is given by the ratio of the slope to the intercept.

Thermal Denaturation. DNA Melting experiments were carried out by monitoring the absorption intensity of CT-DNA (100 μM) at 260 nm in the temp. range of 35–90° with temp. increments of 1°, both in the absence and presence of the Cu^{II} complex (20 μM). Measurements were performed with an *Agilent 8453* UV/VIS spectrophotometer. The melting temperature (T_m) of DNA was determined as the midpoint of the optically detected transition curves. The ΔT_m value was defined as the difference between T_m of the free DNA and T_m of the bound DNA.

DNA Cleavage. For the gel-electrophoresis experiments, supercoiled pUC19 DNA (300 μg ml^{-1}) was treated with Cu^{II} complexes (200 μM) in 50 mM *Tris*, 18 mM NaCl buffer, pH 8.0, and the solns. were incubated for 1 h in the dark, then irradiated at r.t. Reactions were allowed to proceed for 3 h at 37°. All reactions were quenched by addition of 5 μl of loading buffer (40% sucrose, 0.2% bromophenol blue). The aliquots were loaded on to 1% agarose gel and submitted to electrophoresis at 50 V in *1X TAE* buffer. Gel was stained with 0.5 μg/ml ethidium bromide (EB) and photographed on UV illuminator. The percentage of each form of DNA was quantified using *AlphaDigiDoc*™ RT. Version V.4.1.0 PC-Image software.

Superoxide Dismutase (*SOD*). The SOD activity was evaluated using the nitroblue tetrazolium (NBT) assay according to the following scheme [53].

$$O_2 \xrightarrow{\text{PMS/NADH}} O_2^{\bullet-} \xrightarrow{\text{NBT}} \text{blue formazan} \tag{2}$$

Superoxide anions are produced from the NBT/NADH/PMS system. The indicator utilized in this case is NBT, which reacts with $O^{\bullet-}_2$ to form blue formazan. The SOD model complex, added to the soln., inhibits the reaction by reacting with superoxide directly. The value of inhibition can thus be used to determine activity of the SOD model complex.

Nonenzymatic system containing 30 μM PMS, 79 μM NADH, and 75 μM NBT, phosphate buffer (pH 7.8) was used to produce superoxide anion ($O^{\bullet-}_2$) and the scavenging rate of $O^{\bullet-}_2$ was determined by monitoring reduction rate of transformation of NBT to monoformazan dye under the influence of 0.25–3.0 μM tested compound [45]. The concentration of the complex required to attain 50% inhibition of the reduction (defined as IC_{50}) was determined as an indication of SOD-like activity. The reactions were monitored at 560 nm with a UV/VIS spectrophotometer, and the rate of absorption change was determined. The % inhibition of NBT reduction was calculated using following equation.

$$\%\ \text{inhibition of NBT reduction}=(1-k'/k)\times 100 \tag{3}$$

where k' and k are the slopes of the straight line of absorbance values as a function of time in the presence and absence of SOD mimic compound, resp. The IC_{50} value of the complex was determined by plotting the percentage of inhibition of NBT reduction *vs.* the increase in concentration of the complex. The concentration of the complex which causes 50% inhibition of NBT reduction is defined as IC_{50}.

Cytotoxicity. Brine shrimp (*Artemia* cysts) eggs were hatched in a shallow rectangular plastic dish (22 × 32 cm), filled with artificial seawater, which was prepared with commercial salt mixture and double

dist. H_2O. An unequal partition was made in the plastic dish with the help of a perforated device. Approximately 50 mg of eggs were sprinkled into the large compartment and was opened to ordinary light. After 2 d, nauplii were collected by a pipette from the lighted side. A sample of the test compound was prepared by dissolving 10 mg of each compound in 10 ml of DMSO. From these stock solns., solns. were transfered to 18 vials to make final concentration 2, 4, 8, 12, 16, and 20 μg ml^{-1} (three sets for each dilutions were used for each test sample and mean of three sets was used for LC_{50} calculation), and three vials were kept as control having same amount of DMSO only. When the nauplii were ready, 1 ml of seawater and 10 shrimps were added to each vial, and the volume was adjusted with seawater to 2.5 ml per vial. After 24 h, the number of survivors (*Supplementary Table*[1])) was counted [46]. Data were analyzed by simple logit method to determine the LC_{50} values (*Table 4*), in which log of concentration of samples were plotted against percentage of mortality of nauplii [54].

REFERENCES

[1] F. Mancin, P. Scrimin, P. Tecilla, U. Tonellato, *Chem. Commun.* **2005**, 2540.
[2] A. M. Pyle, E. C. Long, J. K. Barton, *J. Am. Chem. Soc.* **1989**, *111*, 4520.
[3] A. Sitlani, E. C. Long, A. M. Pyle, J. K. Barton, *J. Am. Chem. Soc.* **1992**, *114*, 2303.
[4] L. Jin, P. Yang, *Polyhedron* **1997**, *16*, 3395.
[5] Y.-M. Song, X.-L. Lu, M.-L. Yang, X.-R. Zheng, *Transition Met. Chem.* **2005**, *30*, 499.
[6] I. Fridovich, *Annu. Rev. Biochem.* **1975**, *44*, 147.
[7] H. Koga, A. Itoh, S. Murayama, S. Suzue, T. Irikura, *J. Med. Chem.* **1980**, *23*, 1358.
[8] I. Turel, *Coord. Chem. Rev.* **2002**, *232*, 27.
[9] 'Quinolone Antimicrobial Agents', 3rd edn., Eds. D. C. Hooper, E. Rubinstein, ASM Press, Washington, DC, 2003.
[10] 'The Quinolones', 3rd edn., Ed. V. T. Andriole, Academic Press, San Diego, CA, 2000.
[11] D. T. W. Chu, P. B. Fernandes, in: 'Advances in Drug Research', Vol. 21, Ed. B. Testa, Academic Press, London, 1991, pp. 39.
[12] 'Martindale: The Extra Pharmacopeia', 30th edn., Ed. J. E. F. Reynolds, The Pharmaceutical Press, London, 1993, pp. 145–147.
[13] H. C. Neu, *Am. J. Med.* **1989**, *87*, S1.
[14] R. E. Polk, *Am. J. Med.* **1989**, *87*, S76.
[15] M. J. e Souza, C. F. Bittencourt, L. M. Morsch, *J. Pharm. Biomed. Anal.* **2002**, *28*, 1195.
[16] M. Scheer, *Vet. Med. Rev.* **1987**, *2*, 90.
[17] J.-Y. Fan, D. Sun, H. Yu, S. M. Kerwin, L. H. Hurley, *J. Med. Chem.* **1995**, *38*, 408.
[18] S. Dessus-Babus, C. M. Bébéar, A. Charron, C. Bébéar, B. De Barbeyrac, *Antimicrob. Agents Chemother.* **1998**, *42*, 2474.
[19] S. Ameyama, Y. Shinmura, M. Takahata, *Antimicrob. Agents Chemother.* **2003**, *47*, 2327.
[20] A. D. Kulkarni, S. A. Patil, P. S. Badami, *Int. J. Electrochem. Sci.* **2009**, *4*, 717.
[21] A. B. P. Lever, 'Inorganic Electronic Spectroscopy', 2nd Edn., Elsevier, Amsterdam, 1984.
[22] B. N. Figgis, R. S. Nyholm, D. Nasipuri, B. E. Betts, W. Davey, M. A. P. Hogg, J. E. Spice, E. Boyland, P. Sims, M. M. Coombs, J. Lamy, D. Lavit, N. P. Buu-Hoï, S. J. W. Price, A. F. Trotman-Dickenson, D. J. Alner, A. G. Smeeth, W. Tadros, A. B. Sakla, M. S. Ishak, F. C. Cooper, C. L. Arcus, P. A. Hallgarten, D. A. H. Taylor, *J. Chem. Soc.* **1958**, 4190.
[23] G. B. Deacon, R. J. Phillips, *Coord. Chem. Rev.* **1980**, *33*, 227.
[24] C. Dendrinou-Samara, G. Tsotsou, L. V. Ekateriniadou, A. H. Kortsaris, C. P. Raptopoulou, A. Terzis, D. A. Kyriakidis, D. P. Kessissoglou, *J. Inorg. Biochem.* **1998**, *71*, 171.
[25] P. B. Pansuriya, P. Dhandhukia, V. Thakkar, M. N. Patel, *J. Enzyme Inhib. Med. Chem.* **2007**, *22*, 477.
[26] M. N. Patel, P. A. Parmar, D. S. Gandhi, *J. Enzyme Inhib. Med. Chem.* **2011**, *26*, 188.
[27] H. H. Freedman, *J. Am. Chem. Soc.* **1961**, *83*, 2900.
[28] Z. H. Chohan, *Appl. Organomet. Chem.* **2006**, *20*, 112.

---

[1]) *Supplementary Material* is available from the corresponding author.

[29] Z. H. Chohan, M. Arif, Z. Shafiq, M. Yaqub, C. T. Supuran, *J. Enzyme Inhib. Med. Chem.* **2006**, *21*, 95.
[30] H. Chao, W.-J. Mei, Q.-W. Huang, L.-N. Ji, *J. Inorg. Biochem.* **2002**, *92*, 165.
[31] F. Gao, H. Chao, F. Zhou, Y.-X. Yuan, B. Peng, L.-N. Ji, *J. Inorg. Biochem.* **2006**, *100*, 1487.
[32] D.-S. Guo, X.-Y. Yuan, J.-B. Wu, *J. Inorg. Biochem.* **2007**, *101*, 644.
[33] G. Psomas, *J. Inorg. Biochem.* **2008**, *102*, 1798.
[34] A. Tarushi, C. P. Raptopoulou, V. Psycharis, A. Terzis, G. Psomas, D. P. Kessissoglou, *Bioorg. Med. Chem.* **2010**, *18*, 2678.
[35] A. Tarushi, G. Psomas, C. P. Raptopoulou, D. P. Kessissoglou, *J. Inorg. Biochem.* **2009**, *103*, 898.
[36] S. Satyanarayana, J. C. Dabrowiak, J. B. Chaires, *Biochemistry* **1992**, *31*, 9319.
[37] S. Satyanarayana, J. C. Dabrowiak, J. B. Chaires, *Biochemistry* **1993**, *32*, 2573.
[38] M. J. Waring, *J. Mol. Biol.* **1965**, *13*, 269.
[39] G. A. Neyhart, N. Grover, S. R. Smith, W. A. Kalsbeck, T. A. Fairly, M. Cory, H. H. Thorp, *J. Am. Chem. Soc.* **1993**, *115*, 4423.
[40] L. N. Ji, X. H. Zou, J. G. Liu, *Coord. Chem. Rev.* **2001**, *216–217*, 513.
[41] A. Sitlani, E. C. Long, A. M. Pyle, J. K. Barton, *J. Am. Chem. Soc.* **1992**, *114*, 2303.
[42] D. S. Sigman, *Acc. Chem. Res.* **1986**, *19*, 180.
[43] R. R. Sinden, 'DNA Structure and Function', Academic Press Limited, London, 1994, pp. 131–133.
[44] J. Casanova, G. Alzuet, J. Borrás, J. Latorre, M. S. Sanaú, S. García-Granda, *J. Inorg. Biochem.* **1995**, *60*, 219.
[45] I. Fridovich, in: 'CRC Handbook of Methods for Oxygen Radical Research', Ed. R. A. Greenwald, CRC Press, Boca Raton, FL, 1985, p. 51.
[46] B. N. Meyer, N. R. Ferrigni, J. E. Putnam, L. B. Jacobsen, D. E. Nichols, J. L. McLaughlin, *Planta Med.* **1982**, *45*, 31.
[47] B. Jaki, J. Orjala, H.-R. Bürgi, O. Sticher, *Pharm. Biol.* **1999**, *37*, 138.
[48] A. I. Vogel, 'Textbook of quantitative inorganic analysis', 4th ed., ELBS and Longman, London, 1978.
[49] L. J. Henderson Jr., F. R. Fronczek, W. R. Cherry, *J. Am. Chem. Soc.* **1984**, *106*, 5876.
[50] S. Trofimenko, *J. Am. Chem. Soc.* **1970**, *92*, 5118.
[51] J. B. Chaires, N. Dattagupta, D. M. Crothers, *Biochemistry* **1982**, *21*, 3933.
[52] G. Cohen, H. Eisenberg, *Biopolymers* **1969**, *8*, 45.
[53] A. Wolfe, G. H. Shimer Jr., T. Meehan, *Biochemistry* **1987**, *26*, 6392.
[54] M. R. Islam, S. M. R. Islam, A. S. M. Noman, J. A. Khanam, S. M. M. Ali, S. Alam, M. W. Lee, *Mycobiology* **2007**, *35*, 25.

Received November 9, 2011